Evolution of hot rolling texture in pure tungsten and lanthanum oxide doped tungsten with various reductions
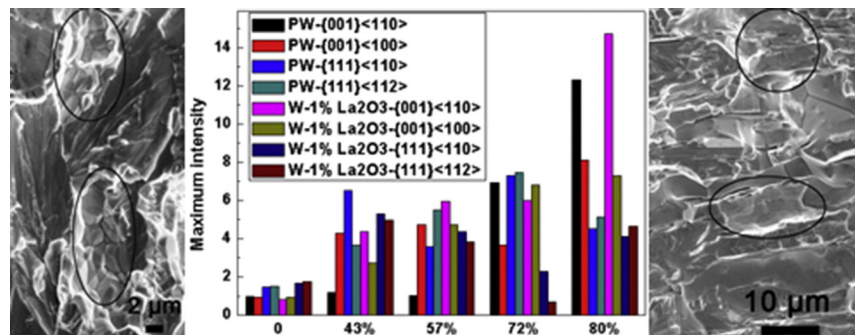
Xiaoxin Zhang, Qingzhi Yan *, Shaoting Lang, Yijia Wang, Changchun Ge

30 Xueyuan Road, Haidian District, Institute of Nuclear Materials, University of Science & Technology Beijing, Beijing, China

HIGHLIGHTS

- Hot rolled PW and W-1%La$_2$O$_3$ with various strains displayed θ-fiber and γ-fiber textures simultaneously
- Dynamic recovery in 72% rolled PW, 43% rolled W-1%La$_2$O$_3$ improved {001}⟨110⟩ texture
- Dynamic recrystallization in 80% rolled PW, 72% rolled W-1%La$_2$O$_3$ improved {001}⟨100⟩ texture and reduced {111}⟨112⟩ texture
- Occurrence of dynamic recovery and dynamic recrystallization in W-1%La$_2$O$_3$ was sooner than in PW

GRAPHICAL ABSTRACT

ARTICLE INFO

ABSTRACT

Textures of hot rolled pure tungsten (PW) and W-1.0 wt%La$_2$O$_3$ (W-1%La$_2$O$_3$) with various strains were characterized to figure out the effect of rolling reduction and second phase on evolution of hot rolling texture. Initial sintering texture of ⟨111⟩//ND and {110}⟨111⟩, {112}⟨111⟩ slip systems as well as dynamic recovery, dynamic recrystallization facilitated the formation of the θ-fiber and γ-fiber textures for PW and W-1%La$_2$O$_3$ during the hot rolling process. Furthermore, dynamic recovery occurred in 72% rolled PW and 43% rolled W-1%La$_2$O$_3$ led to a significant rise of {001}⟨110⟩ texture. Besides, dynamic recrystallization occurred in 80% rolled PW and 72% rolled W-1%La$_2$O$_3$ resulted in an enhancement of {001}⟨100⟩ accompanied with a drop of {111}⟨112⟩ texture. The occurrence of dynamic recovery and dynamic recrystallization in W-1%La$_2$O$_3$ was sooner than in PW, which may be caused by more dislocations in total and additional geometrically necessary dislocations as well as local deformation zone induced by adding of La$_2$O$_3$ particles.

© 2016 Published by Elsevier Ltd.

1. Introduction

Tungsten (W) and its alloys exhibit a range of desirable properties such as high melting point, high thermal conductivity, high density, high modulus of elasticity, high recrystallization temperature, excellent high temperature mechanical properties, low vapor pressure, low thermal expansion and so on [1,2]. As such, W and its alloys have been applied in many fields, such as lighting engineering, electronics industry, manufacturing industry, aerospace field, military field, medical field and nuclear field [3–7]. So various properties are desired for these different applications and the properties are influenced by the crystallographic texture significantly [8]. For example, irradiation resistance [9–14], surface modification induced by particle bombardment [15–17] fracture toughness [18], ductile-brittle transition temperature [18] and particle, energy reflection coefficient [19] of W highly depends

upon the crystal orientation. Thus the investigation of texture characteristics for W is necessary and significant.

Previous literatures more focused on the texture of W wire [20–23], W coating [24], cold rolled W sheet [25,26] and recrystallized W [26,27]. Whereas hot rolling texture of W was rarely reported in detail except for [28], which evaluated the effect of reduction on the hot rolling texture development of pure W (PW). Rolling reduction and second phase are the main factors influencing the strength of the textures and the balance between the various texture components [29]. Thus hot rolling texture characteristics of W were evaluated taking rolling reduction and second phase into account simultaneously in the present paper. Hot rolled PW samples with various strains were also prepared for comparison. Besides, Electron Back-Scattered Diffraction (EBSD) is usually used to measure the single or several grain orientations while X-ray Diffraction (XRD) can measure the sum of grain orientation in large zones. So EBSD and XRD are more suitable to determine the micro-texture and macro-texture, respectively [30]. Therefore, hot rolling textures of PW and W-1.0wt%La$_2$O$_3$ (W-1%La$_2$O$_3$) sheets with various reductions were characterized by XRD to determine the effect of rolling reduction and second phase on the texture development simultaneously in the present paper.

2. Materials and methods

2.1. Material and rolling experiments

The starting PW and W-1%La$_2$O$_3$ powders with grain size of about 3 μm was commercial. Chemical compositions of the PW and W-1%La$_2$O$_3$ powders are shown in Table 1. Then the W powders were pressed to about 55% of the theoretical density, presintered at about 1473 K for 40 min and sintered at about 2373 K for 2 h. On the basis of our experience, the optimum relative density of the sintered W billet to avoid cracking during the following rolling process was in the range of 92%–94%, which can be achieved by medium-frequency induction sintering at 2373 K for 2 h. The relative density was 92.8% for the sintered PW and 92.5% for the sintered W-1%La$_2$O$_3$. Subsequently, the 28-mm-thick PW and W-1%La$_2$O$_3$ billets were unidirectional rolled to 16, 12, 7.8, 5.6 mm, respectively. The maximum initial thickness of 28 mm was limited by the rolling equipment. The minimum final thickness of 5.6 mm was limited by the specimen size for mechanical property tests and achieved after 8 passes rolling. 16, 12 and 7.8-mm-thick W plates underwent 2, 4 and 6 passes rolling, respectively. Finally, these deformed sheets were annealed at 1373 K in hydrogen atmosphere for 2 h to relax residual stresses. Samples for texture measurement and microstructure examination were sectioned along the final rolling direction and the texture measurement specimens were cut from the RD-TD surface and the microstructure examination specimens were cut from the RD-ND surface, respectively. RD, TD and ND are short for rolling direction, transverse direction and normal direction, respectively.

2.2. Characterization

Texture measurement tests were conducted by XRD technique. The textures were examined by measuring the three incomplete pole figures {110}, {200}, {211} in the center layer (RD-TD plane) of the

Fig. 1. Schematic illustration of important fibers in the BCC materials.

samples. The measurements were carried out in the range of the pole distance angle from 20° to 90° in the back reflection mode using Cu Kα1 radiation. During the measurements, the specimens were oscillated along the TD to cover a larger specimen area. The Orientation Distribution Functions (ODFs) were computed from the above three pole figures. Before texture measurement, specimen surface (15 × 15 mm^2) was mechanical polished. Fracture surface morphology was examined by scanning electron microscopy (SEM) to determine the microstructure characteristics, especially the dynamic recrystallization microstructure. Fracture surface was obtained by three-point bending (3 PB) test, which was conducted at room temperature and constant loading rate of 0.5 mm/min on the specimens of 3 × 4 × 35 mm^3 with working span of 30 mm and the length orientation (35 mm) parallel to the rolling direction.

3. Results

Firstly, the ideal orientations of texture components in BCC metals are shown schematically in Fig. 1 [31] and Table 2 [31]. The most relevant texture fibers for BCC materials are [29–34] as follows:

(1) θ-Fiber (crystallographic fiber axis ⟨001⟩ parallel to the normal direction, including major components: {001}⟨100⟩; {001}⟨110⟩).

Table 1
Chemical compositions of the PW and W-1%La$_2$O$_3$ powders, ppm.

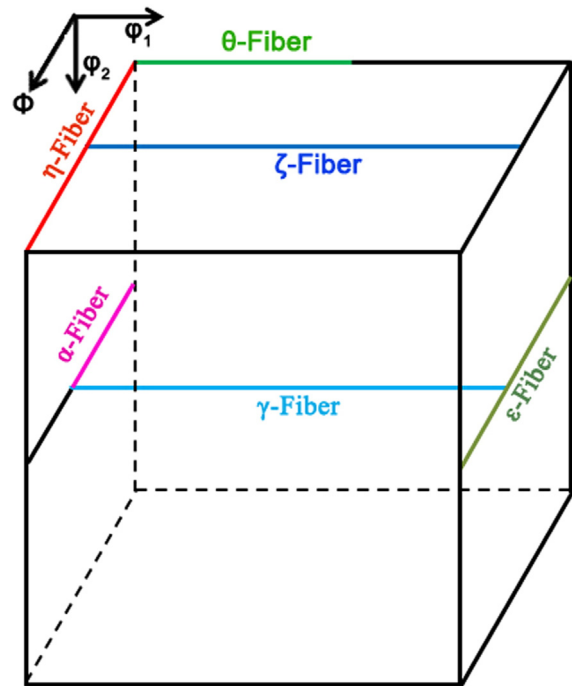| |
|---|
| PW: O < 380, C < 26, Mo < 14, Fe < 10, K < 5, Cr < 6, Si < 6, Ni < 7, Ca < 6, As < 7, S < 5, Na < 5, P < 5, Mg < 2, Al < 2, Sb < 1, V < 2, Mn < 2, Co < 2, Sn < 1, Pb < 1, Cu < 3 |
| W-1%La$_2$O$_3$: C < 19, Mo < 16, Fe < 10, K < 10, Cr < 10, Si < 7, Ni < 7, Ca < 6, As < 6, S < 5, Na < 5, P < 5, Mg < 2, Al < 2, Sb < 2, V < 2, Mn < 2, Co < 2, Sn < 1, Pb < 1, Cu < 1 |

Table 2
Euler angles and Miller indices for important textures in the BCC metals.

Texture components	Euler angles			Fiber
	φ_1	Φ	φ_2	
{001}⟨100⟩	0	0	0	η/θ
{001}⟨110⟩	45	0	0	θ
{011}⟨100⟩	0	45	0	η/ζ
{011}⟨011⟩	90	45	0	ζ
{011}⟨211⟩	35	45	0	ζ
{011}⟨111⟩	55	45	0	ζ
{111}⟨112⟩	30	55	45	γ
{111}⟨110⟩	0	55	45	α/γ
{112}⟨110⟩	0	35	45	α